

Evaluation of the risk of pollution in areas favorable to the realization of productive boreholes in the department of Yamoussoukro (Central Ivory Coast)

Evaluation du risque de pollution des zones favorables à l'implantation de forages productifs dans le département de Yamoussoukro (Centre de la Côte d'Ivoire)

Kamenan Yiwa MONIQUE¹, Kouadio Kouamé Jean OLIVIER^{2*}, Mangoua OiMangoua JULES¹, Fatoumata MEITE¹, Dibi BROU¹, Konan-Waidhet Arthur BRICE¹.

1. Laboratory of Science and Technology of Environment, Jean Lorougnon Guédé University, Daloa, (Côte d'Ivoire).

2. Geology and Mineral Resources Laboratory, Félix Houphouët-Boigny University, Abidjan (Côte d'Ivoire). 5* olivierkouame05@gmail.com.

Abstract. Groundwater resources, although considered safe because they are supposed to be pollution-free, are threatened by various sources of point and diffuse pollution. This study aims to investigate the vulnerability to pollution of groundwater storage areas in the Yamoussoukro department. This study was carried out using hydro-climatic and hydrogeological data and satellite images. GIS combined with remote sensing and Multiple Influence Factors (MIFs) was used to identify groundwater storage areas and map vulnerability to pollution using the PaPRI method. The results show that the Yamoussoukro department has significant groundwater reserves, covering 67% of its surface area. The results obtained from mapping vulnerability to pollution reveal three (3) classes of vulnerability: moderate (28.2%), high (71.3%) and very high (0.5%). This predominance of the high class (71%) shows that groundwater in the Yamoussoukro department is exposed to a high risk of pollution.

Keywords: Fissured aquifer, Groundwater, Pollution, Vulnerability, Yamoussoukro (Central Ivory Coast).

Résumé. Les ressources en eau souterraine, bien que considérées comme sûres car censées être exemptes de toutes les pollutions, sont menacées par diverses sources de pollution ponctuelle et diffuse. Cette étude a pour objectif d'étudier la vulnérabilité à la pollution des zones de stockage des eaux souterraines dans le département de Yamoussoukro. Cette étude a été réalisée avec des données hydro-climatiques, hydrogéologiques et des images satellites. Le SIG combiné à la télédétection et aux facteurs d'influence multiples (FIM) a été utilisé pour identifier les zones de stockage des eaux souterraines et cartographier leur vulnérabilité à la pollution en utilisant la méthode PaPRI. Les résultats de cette étude montrent que le département de Yamoussoukro dispose d'importantes réserves d'eau souterraine, couvrant environ 67% de sa superficie totale. Les résultats obtenus à partir de la cartographie de la vulnérabilité à la pollution révèlent trois (3) classes de vulnérabilité: modérée (28,2 %), élevée (71,3 %) et très élevée (0,5 %). Cette prédominance de la classe élevée (71 %) montre que les eaux souterraines du département de Yamoussoukro sont exposées à un risque élevé de pollution.

Mots-clés : Aquifère fissuré, Eau souterraine, Pollution, Vulnérabilité, Yamoussoukro (Centre de la Côte d'Ivoire).

INTRODUCTION

In 2011, according to the World Health Organization (WHO), more than 2 million people, mostly children under the age of five in developing countries where hygiene and sanitation measures are inadequate, died each year from diarrheal diseases, 90% of which are attributable to the poor quality of drinking water (Kouassi *et al.* 2017). In Côte d'Ivoire, the major urban centers located in bedrock zones are supplied with drinking water by surface water, which is an abundant and perennial resource (Ahoussi 2008, Dibi 2008). Yet these surface water resources are becoming increasingly scarce and degraded due to the adverse effects of climate change, population growth and various forms of anthropogenic pollution (Mahe *et al.* 2001, Koffi *et al.* 2021, 2023). In these areas, drinking water supplies are therefore directed towards alternative sources such as groundwater from deep aquifers, the quality of which generally meets WHO guidelines (Biémi 1992). This is also the case in the department of Yamoussoukro, where population growth in recent years could increase the population's need for water

and upsurge the risk of pollution. As a result, other sources of drinking water, such as water from fissured aquifers in the area, need to be identified and measures taken to protect these resources. To this end, long-term planning objectives for the management of this resource suggest looking at its intrinsic vulnerability, given that it can be considered invariant over time (Dibi *et al.* 2013). It was against this backdrop that studying the vulnerability of groundwater storage areas in the Yamoussoukro department to pollution was initiated.

Study area

The department of Yamoussoukro is located in central Côte d'Ivoire, between longitudes 4°40' and 5°33' West and latitudes 6°13' and 7°06' North. This department covers the autonomous district of Yamoussoukro, comprising four sub-prefectures: Yamoussoukro, Kossou, Attiégoakro, and Lolobo, covering a surface area of around 1.268 km² (Fig. 1). The Yamoussoukro department had a population of around 422.072 in 2021 (INS 2021). Like Côte d'Ivoire as a whole, the Yamoussoukro department is experiencing a high annual population growth rate of around 3% from 2014 to 2021.

The Yamoussoukro department belongs to the granitic-gneissic peneplain of the Precambrian basement. The main geological formations are made up of igneous and metamorphic rocks. Igneous rocks occupy 88.7% of the study area. These rocks belong to the Eburnean complex and include Eburnean granitoids. They are biotite granites, two-mica granites, migmatites, concordant granodiorites, diorites, and gneisses (N'guessan *et al.* 2014). These two main geological formations give rise to a hydrogeological context characterized by an alterite aquifer and a fissured or fractured aquifer.

MATERIALS AND METHODS

Data

Several types of data were required for this study:

- hydrogeological data supplied by the Regional Directorate of Hydraulics (RDH) in the study area. These consist of borehole data sheets and pumping tests from 60 boreholes throughout the study area;

- satellite images consisting of the 30 m × 30 m resolution Digital Terrain Model (DTM) used to produce the slope map, drainage density map and elevation map, and the 197-055 scene used to produce the fracturing and fracturing density map;

- rainfall data provided by the Airport, Aeronautical and Meteorological Operations and Development Company, for the period 1990-2020, which were used to produce the rainfall map.

Methodology

Identification of potential groundwater storage areas

1. Definition of basic criteria for identifying potential groundwater storage areas

The quantitative indicators involved in mapping groundwater resources can be grouped into three main

groups: These are availability, exploitability and accessibility (Kanohin 2010, Mangoua *et al.* 2014).

- The availability indicator reflects the notion of the existence of an aquifer and is the first condition to be known before any other activity (Savané 1997). It results from the combination of parameters such as slope, drainage density, fracture density, weathering thickness and effective infiltration. Effective infiltration is the most important parameter for groundwater availability (Yao *et al.* 2016).

- The operability indicator depends on the operating flow rate and the static level of the water table. The operating rate is conditioned by the quantity of water in the groundwater reserve, but also by how quickly this reserve can be replenished in the event of heavy demand (Youan Ta *et al.* 2011).

- The accessibility indicator provides information on access conditions to groundwater resources. These conditions are considered to be economic and social factors, as they may or may not favor access to the resource. The main accessibility factors are drilling depth and success index.

2. Criteria weighting

Weighting is the process of assigning weights to each criterion for the achievement of a given indicator. The value of the weights is relative to the importance of the criterion in the achievement of the phenomenon reflected by the indicator. In this study, weighting was carried out using the Analytical Hierarchy Process (AHP) pairwise comparison method developed by (Saaty 2008). It enables the production of standardized weighting coefficients whose sum is equal to 1.

This method consists of making a pairwise comparison of the criteria for a given indicator, then assigning a comparison score (Tab. 1) to each criterion according to its importance in achieving the given indicator.

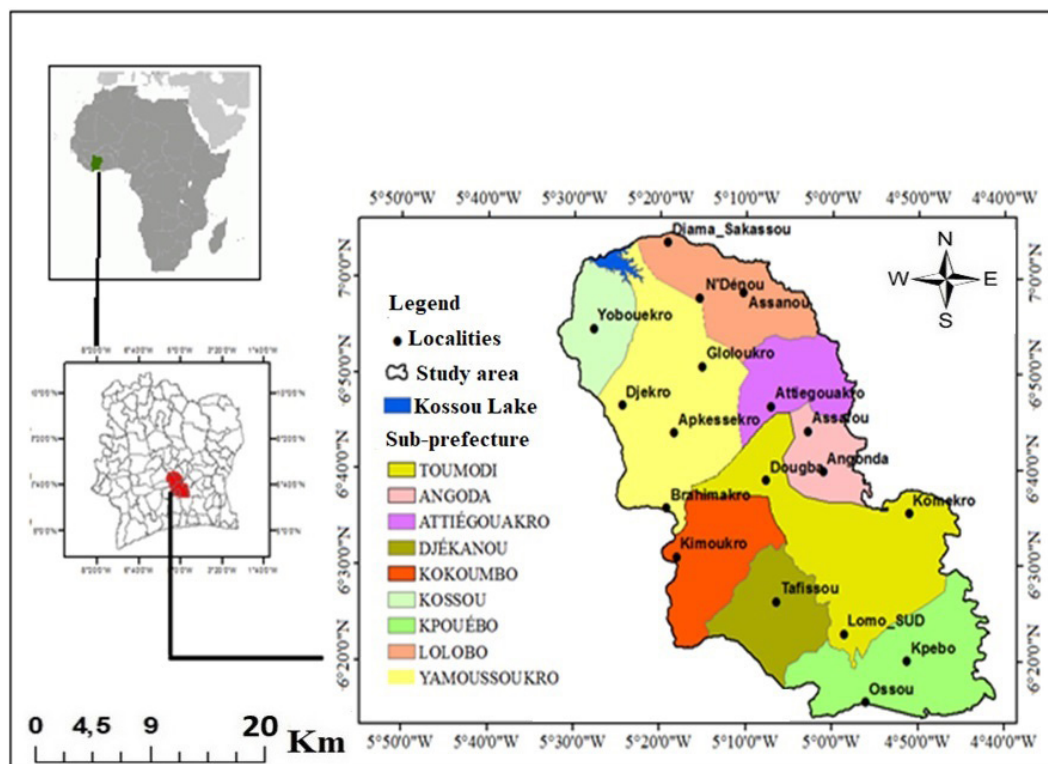


Figure 1. Study area of the department of Yamoussoukro in the Central Ivory Cost.

Table 1. Verbal and numerical expression of the relative importance of a pair of criteria (El Morjani 2003).

Expressing one criterion about another	Score
Same importance	1
Moderately important	3
Highly important	5
Very important	7
Extremely important	9
Moderately less important	1/3
Less important	1/5
Significantly less important	1/7
Extremely less important	1/9

In the case of this study, the pairwise comparison matrices and criteria weights for each indicator and for the three indicators are presented (Tab. 2-3).

3. Criteria aggregation

In this study, the method of aggregating criteria by weighting was used. This consists in summing the standardized and weighted values of each criterion involved in the construction of a given indicator. The final result (S) representing the value of the indicator is given by equation 1:

$$S = \sum_{i=1}^n w_i x_i \quad (\text{Eq. 1})$$

With S: the result; w_i the weight of criterion i ; and x_i the standardized value of criterion i .

Aggregation by weighting provides a suitability index on a scale from 0 to 10. Indeed, the sum of the weighting coefficients generated by Saaty's (2008) method is 1. Mapping a given indicator involves plotting in a geographical space the various values obtained by summing the standardized and weighted values of each criterion used to construct the indicator (Youan Ta *et al.* 2011). A reclassification of the indicators will lead to thematic maps with four classes: poor, mediocre, good and excellent. The number of classes has

been fixed at four for better legibility and interpretation of the resulting map.

4. Validation of the various thematic maps

The thematic maps produced were validated by calculating uncertainty (Doumouya *et al.* 2012). Validation of these maps based on previous studies showed certain shortcomings (Youan Ta *et al.* 2011).

In fact, it is virtually impossible to find a sensitivity class that reflects 100% of the reality in the field, because next to a borehole with a high flow rate, it is possible to have another borehole with a low flow rate. For this reason, the uncertainties on the averages of the various parameters of the main indicators have been calculated based on equation 2:

$$\Delta \bar{X} = \frac{\sigma}{\sqrt{m}} \quad (\text{Eq. 2})$$

$\Delta \bar{X}$: uncertainty about the mean of the data series;
 σ : standard deviation of the data series ;
 m : number of data.

An expansion factor (K) is then calculated to determine the confidence level. The determination of this parameter is based on the statistical principle of calculating expanded uncertainty. The K factor is used to define an interval of sufficient range to attest to the robustness of the results (equation 3):

$$K = \frac{|E - \bar{X}|}{\sigma} \quad (\text{Eq. 3})$$

K is the expansion factor, and E corresponds to the extreme value of the statistical series, which can be the maximum or minimum of the series. Confidence levels for the various parameters were deduced from the different K values. Thus, $K = 1$ for 68% confidence, $K = 2$ for 95% confidence and $K = 3$ for 99% confidence.

Mapping vulnerability to groundwater pollution in the study area

The PaPRI method (Protection of aquifers based on Protection, Reservoir, and Infiltration) was used to map areas vulnerable to pollution in fractured aquifers. This method provides for the consideration of three (3) criteria (Dibi *et al.* 2015). The principle is based on multicriteria analysis, which

Table2. Pair-wise comparison matrix and weighting coefficient for availability indicator criteria.

	Infiltration	DF	Slope	DD	EA	Vp	Wi
Infiltration	1	5	2	7	5	3.23	0.46
DF	1/5	1	1/3	2	5	0.92	0.13
Slope	1/2	3	1	5	5	2.06	0.29
DD	1/7	1/2	1/5	1	1	0.43	0.06
EA	1/5	1/5	1/5	1	1	0.38	0.05

Table3. Pairwise comparison matrix and weighting coefficient for accessibility and exploitability indicator criteria (Youan Ta *et al.* 2011).

Accessibility indicator				
	IS	PF	Vp	Wi
Success Index (SI)	1	1/3	0.58	0.25
Drilling depth	3	1	1.7	0.75
Operability indicator				
	QE	NS	Vp	Wi
Operating Yield	1	3	1.7	0.75
Static level	1/3	1	0.58	0.25

involves studying each criterion separately according to its role in pollution vulnerability analysis, and then a thematic map is drawn up for each of them. The thematic maps of the three (3) criteria are then combined to produce a map of areas vulnerable to pollution. The process is organized into six (6) stages: identification of the criteria, reclassification of the criteria, weighting by multi-criteria analysis, determination of the vulnerability index, determination of the vulnerability classes, and finally validation of the vulnerability map.

1. Identification of criteria

- The Protection (P) criterion represents all the factors that contribute to protecting the water table from infiltration. It characterizes the ability to reduce the transport of pollutants and their rate of transfer from the surface to the water table. It depends on the thickness and nature of the soil (S) stripped before drilling, the alterites (A), depending on the thickness crossed, the unsaturated zone (UZ), taking into account granites and fissured shales as well as fracturing (Dibi *et al.* 2015).

- The Reservoir criterion (R) designates the geological nature of the aquifer reservoir characterized by lithology and fracturing (Dörfleger & Plagnes 2010). The nature of the "roche réservoir" characterizes the degree of permeability of the zone. Fracture density is taken from the detailed fracturing map.

- Infiltration criterion (I) concerns infiltration conditions. It is a function of two parameters: the slope determined from the Digital Terrain Model (DTM) map of the study area and the drainage density obtained from the hydrographic network (Sinan & Razack 2008).

2. Criteria reclassification

The reclassification stage consisted of assigning scores to the different classes of the selected criteria by defining intervals. This process makes it possible to standardize parameters by defining the degree to which each criterion falls within a common interval. Indeed, the strongly unfavorable class always has the lowest score, while the

Table 4. Parameter classification and standardization (Dibi *et al.* 2015).

Criteria	Parameters	Parameter Qualifiers	Class	Score
Protection (P)	Soil (sandyclay)	Low	No soil	4
		Medium	0 - 10 cm	3
		High	10 - 40 cm	2
		Very high	>40 cm	1
	Alterites (m)	Low	0 - 5 m	4
		Medium	5 - 15 m	3
		High	15 - 30 m	2
		Very high	>30 m	1
	Unsaturated zone	Fissuredschists		3
		Fissured granites		2
Reservoir (R)	Nature of the rock	Nature	Very high	Zones of major accidents or open mega-fractures
			High	A loose rock composed of coarse sand and clayey sand
			Medium	Schistes fissurés rencontrés juste au-dessus de la roche saine
			Low	Fissured granites are found just above sound rock
	Fracture density (km/km ²)	Low	1.3 - 1.9	1
		Medium	1.9 - 2.7	2
		High	2.7 - 3.3	3
		Very high	> 3.3	4
Infiltration (I)	Slope (%)	Low	0 - 5 (%)	4
		Medium	5 - 15 (%)	3
		High	15 - 50 (%)	2
		Very high	> 50 (%)	1
	Drainage density (km/km ²)	Low	0.54 - 0.71	4
		Medium	0.71 - 0.93	3
		High	0.93 - 1.23	2
		Very high	> 1.23	1

strongly favorable class has the highest. The result of the reclassification of the identified criteria, whose combination favors good groundwater recharge or not, as well as their matrix of pairwise comparisons, is recorded (Tab. 4).

The synthesis of the various criteria thus presented contributes to the elaboration of the final vulnerability index (Fig. 2).

3. Determination of weighting coefficients

The determination of weighting coefficient according to the PaPRI method is determined on a numerical scale of nine levels defined by El Morjani and modified by Mangoua *et al.* (2018) to have 5 levels as shown (Tab. 5). Based on the calculation of the eigenvector and the weighting coefficient, correlation matrices were drawn up for each sub-criterion to determine the value of the criterion concerned at the level of each mesh.

Table 5. Verbal and numerical expression of the relative importance of a pair of factors (Mangoua *et al.* 2018).

Expressing one criterion about another	Score
Less important	1/3
Slightly less important	1/2
Same importance	1
Slightly higher	2
More important	3

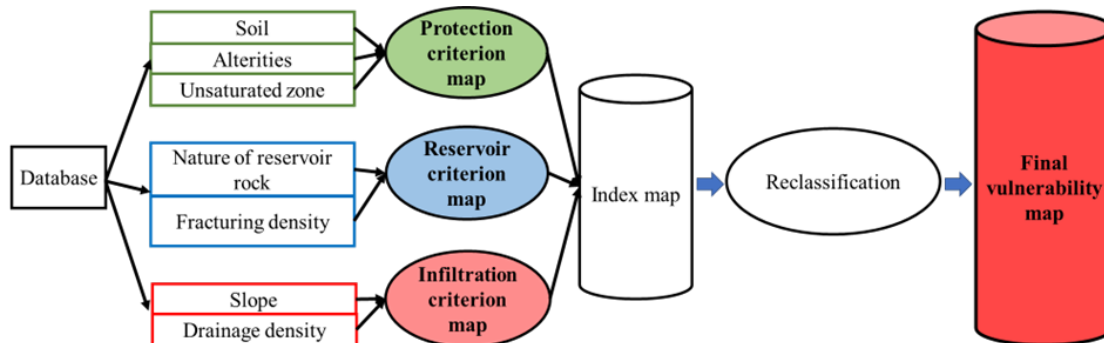


Figure 2. Stages in the development of the vulnerability map (Mangoua *et al.* 2020 modified).

Table 6. Pairwise comparison matrix and weighting of vulnerability factors (Doumouya *et al.* 2012).

Protection (P) factor		Unsaturated zone	Alterites	Soil	Ownvector	Weighting Coefficient
Unsaturatedzone	1	3	3	2.08	0.59	
Alterites	1/3	1	2	0.87	0.25	
Soil	1/3	½	1	0.55	0.16	
Reservoir (R) factor		Fracture density	Nature of Roche	Ownvector	Weighting Coefficient	
Fracture density	1	3	2	0.63		
Nature of Roche	1/3	1	1.15	0.37		
Infiltration (I) factor		Slopes	Drainage density	Ownvector	Weighting Coefficient	
Slopes	1	3	2	0.63		
Drainage density	1/3	1	1.15	0.37		

The values resulting from this comparison (Tab. 6) were then integrated into an eigenvector (equation 8) and weighting coefficient (equation 9) calculation for each parameter (Doumouya *et al.* 2012).

$$V_{Pj} = \sqrt[n]{\prod_{i=1}^n N_i} \quad (\text{Eq.8})$$

V_{Pi} = Eigenvector of each factor; N_i = Value of each factor. The weighting coefficient (W_i) of each factor is determined as follows (equation 9):

$$W_i = \frac{V_{Pj}}{\sum_{i=1}^n V_{Pj}} \quad (\text{Eq.9})$$

(W_i) = weighting coefficient for each factor. On this basis, correlation matrices were drawn up for each sub-criterion to determine the value of the criterion concerned at the level of each mesh.

4. Determining the Vulnerability Index

Calculation of the vulnerability index enables the contours of the protection zones to be estimated. According to Kavouri *et al.* (2011), the most important factor could be infiltration (I), as it is responsible for a high risk of degradation of groundwater quality in these areas. The vulnerability index is therefore determined according to Equation 10:

$$Vg = iI + pP + rR \quad (\text{Eq.10})$$

With I, P and R, the different criteria; i, r and p, the weights of these criteria and Vg , the overall vulnerability index.

5. Determination of Different Vulnerability Class

Five vulnerability classes (Tab.7) were determined and represented by five colors, indicating the degree of index of the criteria at each point in the study area (Dörfliiger & Plagnes 2009).

Table 7. Vulnerability classification (Dörfliiger & Plagnes 2009).

Index of vulnerability	Class	Level of vulnerability
3.2 – 4	4	Very high
2.4 – 3.19	3	High
1.6 – 2.39	2	Moderate
0.8 – 1.59	1	Low
0 – 0.79	0	Very Low

6. Validation of the vulnerability map

In this study, margins of error were used to check the reliability of the pollution vulnerability map. Calculation of the margins of error first requires the determination of the uncertainties in the average indices of the various criteria that make up the method (Dibi *et al.* 2013). Uncertainty is evaluated using equation 11 (Doumouya *et al.* 2012):

$$\Delta\bar{x} = \frac{\sigma}{\sqrt{m}} = \sqrt{\frac{1}{m(m-1)} \sum_{i=1}^m |(x_i - \bar{x})|^2} \quad (\text{Eq.11})$$

With

- $\Delta\bar{x}$: Uncertainty on the average index of each parameter;
- σ : Standard deviation of the vulnerability indices of the hydrogeological parameter;
- m : Number of boreholes considered;
- x_i : Vulnerability index of the hydrogeological parameter at borehole i ;
- \bar{x} : Average vulnerability index of the hydrogeological parameter.

From the uncertainty determined for each parameter, the margin of error itself is calculated from equation 12:

$$E_r = \frac{\Delta\bar{x}}{I_{V-M}} \quad (\text{Eq.12})$$

With I_{V-M} the average vulnerability index for each parameter.

RESULTS

Assessment of various groundwater potential indicators

Areas of good and excellent availability occupy 93.34% of the department's surface area (Fig. 3), while classes of medium and poor availability cover 6.64% and 0.04% of the study area, respectively. The zones of good and excellent availability cover almost the entire area and are characterized by relatively low slopes, high fracture density and moderately low drainage density. They provide favorable conditions for the accumulation of groundwater and, consequently, for the formation of large reserves. In these zones, interconnected open mega-fractures have a high probability of being productive. The groundwater availability map has a margin of error of ± 0.1 with a confidence level of 95%. This means that the groundwater availability map may reflect the realities on the ground.

Good and excellent exploitability classes cover 90.17% of the study area. These zones occupy most of the department and have very high and high exploitation rates. Only 9.83% of the area is classified as medium and poorly exploitable, characterized by very low and low exploitation rates. These

classes are found in pockets on either side of the study area (Fig. 4). The exploitability map has a margin of error of ± 0.1 with a confidence level of 99%. These values attest to the reliability of this thematic groundwater exploitability map could have.

The accessibility map of the department's groundwater resources is characterized by four classes, unevenly distributed over the study area (Fig. 5). Analysis of the map reveals that the poor accessibility class covers only around 6.66% of the department. It is distributed in pockets over almost the entire area. The largest beach is to the south, more precisely in the Tafissou locality. This is an area where most of the negative drilling has been observed. Areas with average accessibility represent around 12% of the department and are located at the western, eastern, and south-western extremities of the Yamoussoukro department. Good and excellent accessibility classes occupy 61% and 20.34% of the area, respectively. On the one hand, these classes cover the greater part of the surface area and, on the other, are divided into pockets located in the Kpouèbo locality, in the central Dougbia locality and also in a few localities in the north. These are generally characterized by medium to shallow boreholes. The accessibility map has a margin of error of ± 0.1 with a confidence level of 99%.

The linear combination of the influencing factors (availability, operability and accessibility) based on their respective weights yielded the map of potential groundwater storage areas in the study area. Fig. 6 shows that this zone is dominated by classes of good and excellent potential. These classes cover around 66% of the area, and are found over almost the entire department, except areas with mediocre and poor classes occupying around 34%, scattered from the extreme left north to the south, and also from the extreme right north to the east. These classes are found in places towards the center and south. Analysis of these different classes reveals that :

- The poor potential class occupies around 9% of the area. These are areas of poor or average availability and accessibility, to which poor harve stability may be added. It is strongly present in the localities of Assanou and N'denou;
- the medium potential class covers around 24% of the study area and occupies zones of poor availability and accessibility, sometimes combined with good exploitability;
- the good water potential class covers a large part of the study area. This class, which is scattered throughout the area, occupies around 42% of the total surface area of the Yamoussoukro department. In these areas, the structures are shallower and more likely to be successful. The water resource is available with a relatively low slope, which allows good groundwater recharge.
- the excellent potential class accounts for around 25%. It is mainly found in the southern part of the region. It is also scattered throughout the department.

The error on the Yamoussoukro department groundwater potential map is ± 0.09 with a confidence level of 99%.

Thematic maps of vulnerability parameters

The thematic map of the protection criterion highlights three protection index classes (low, moderate and high). The study area is dominated by the moderate and high protection classes (Fig. 7), which cover 57.75% and 36.34% of the study area, respectively. These two classes occupy around 94% of the zone. The low protection class occupies the remainder

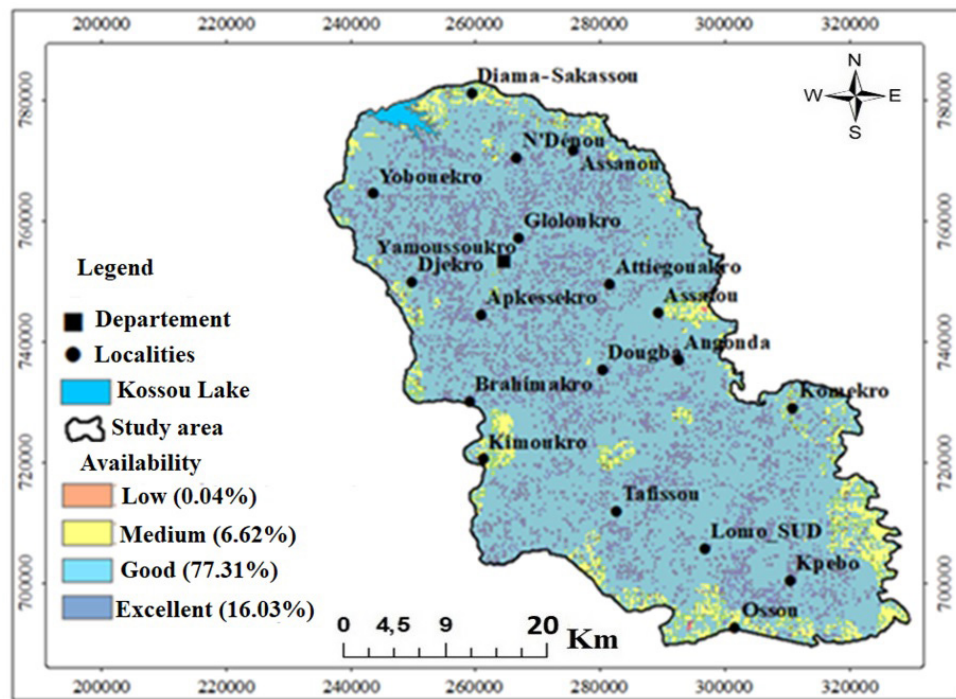


Figure 3. Groundwater availability map of the Yamoussoukro department.

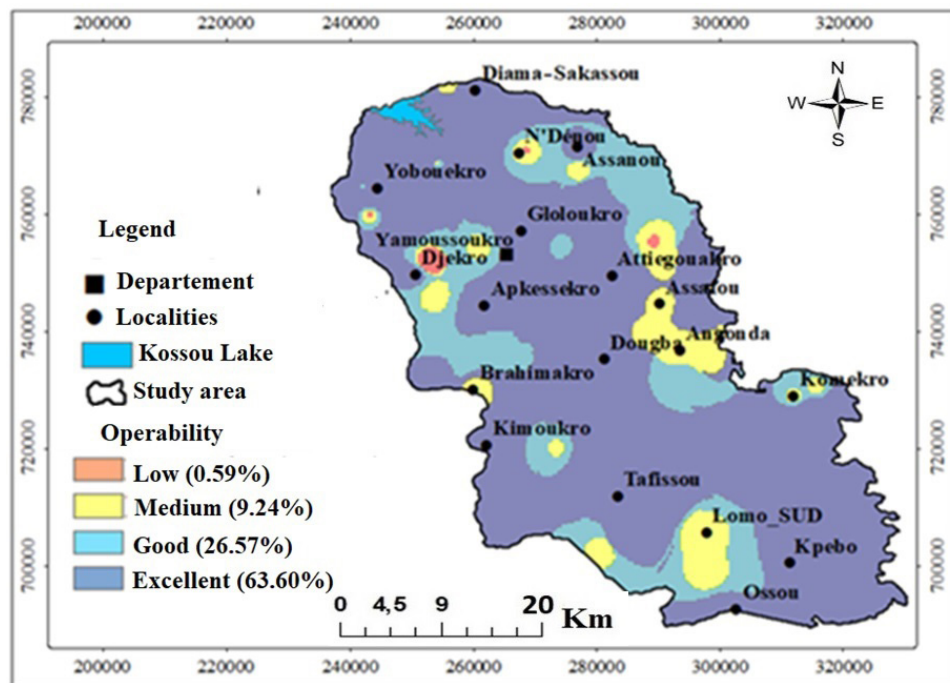


Figure 4. Operability map of groundwater resources in the Yamoussoukro department.

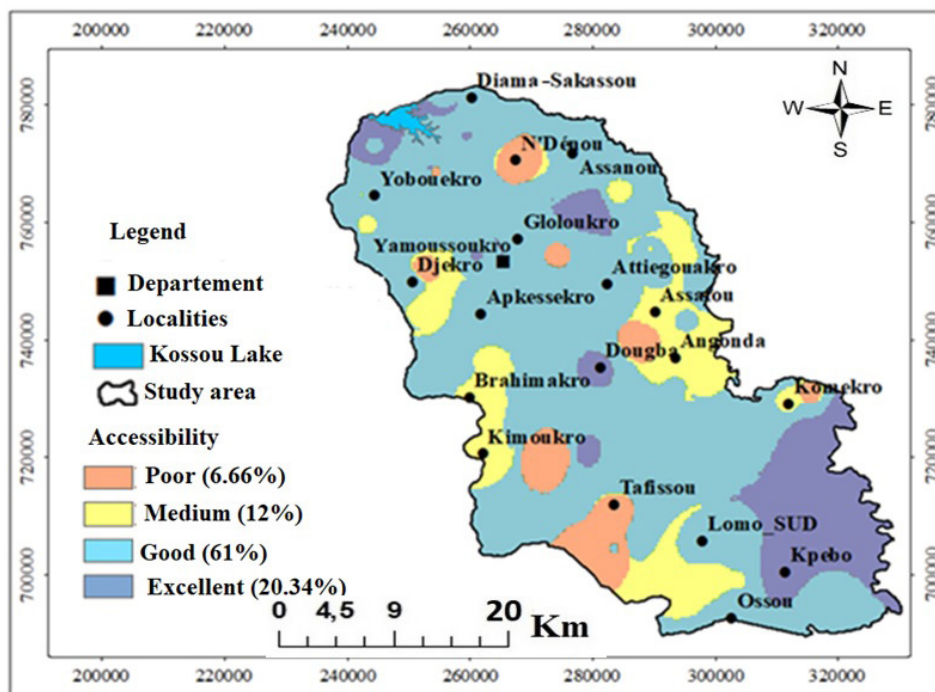


Figure 5. Groundwater accessibility map of the Yamoussoukro district.

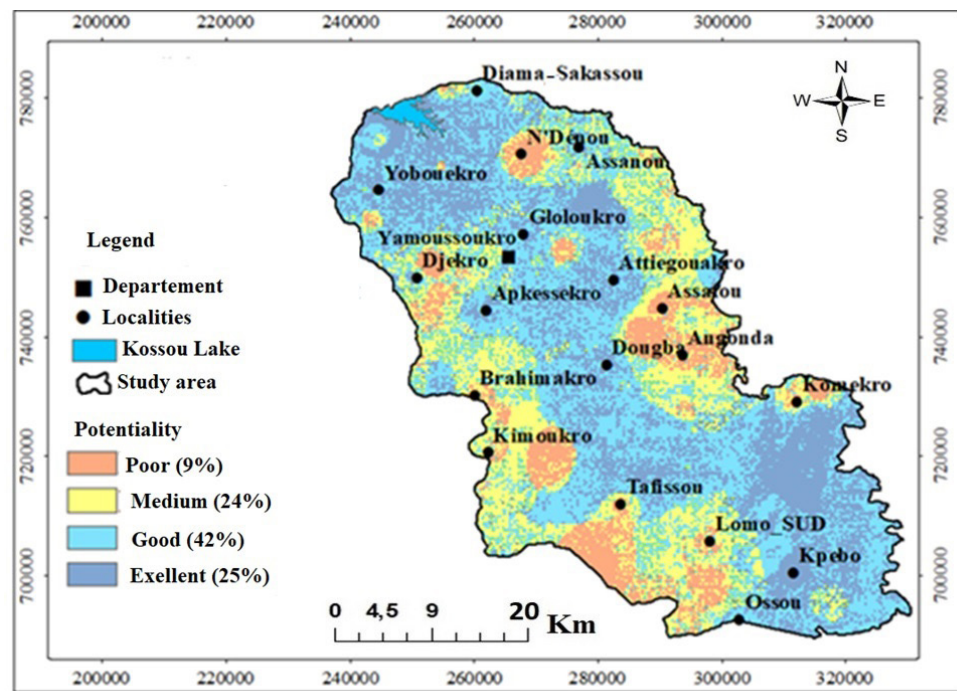


Figure 6. Groundwater potential map of the Yamoussoukro department.

of the zone, with a proportion of 5.91%. It is only found in the north-west of the department. The protection map has a margin of error of 2.3%.

The Reservoir criterion represents the least important criterion in terms of aquifer protection. For this criterion, the higher the degree of permeability, the more vulnerable the aquifer. Analysis of the rock factor results (Fig. 8) shows that the department is dominated by the moderate (59.97%) and low (32.86%) permeability classes. These are found throughout the department except in the area around the zone at two points in the Centre, which are marked by the high and very high permeability class. These are encountered respectively in metamorphic formations of sedimentary or volcanic origin and in undifferentiated ancient crystalline terrain. The high and very high permeability classes cover 7.17% of the study area. The groundwater reservoir criterion map for the Yamoussoukro department has a margin of error of 4.5%.

The infiltration criterion map is dominated by the very high infiltration class (Fig. 9), which occupies 58.34% of the surface area. It occurs over almost the entire study area, with high and moderate infiltration zones occupying 34.93% and 6.73% of the study area, respectively. The groundwater infiltration factor map for the Yamoussoukro department has a margin of error of 2.71%.

Combining all the maps for the Protection, Reservoir and Infiltration criteria, after assigning weights, gives us the overall vulnerability map of aquifers to pollution. The final map (Fig. 10) has the distinctive feature of highlighting areas in need of protection. Analysis of this map shows that the low vulnerability class does not exist in the study area. In fact, the results reveal that the high vulnerability class dominates the department, accounting for at 71.27% of its total surface area. The moderate and very high vulnerability classes occupy 28.19% and 0.54% of the total surface area of the study area, respectively. These sectors are considered to be areas to be monitored. In these areas, intense human activity could pollute groundwater. The error on the groundwater pollution vulnerability map for the Yamoussoukro department is 1.31%.

The error on the map showing vulnerability to groundwater pollution in the department of Yamoussoukro is 1.31%. This map was produced by superimposing the Protection, Reservoir, and Infiltration maps, which have uncertainties of ± 0.04 , ± 0.02 , and ± 0.05 , respectively (Table 8).

Discussion

The use of GIS and multi-criteria analysis in the Yamoussoukro department has resulted in the production of a map of potential groundwater storage areas. Analysis of this groundwater potential map shows that the study area has good and excellent groundwater availability (67% of

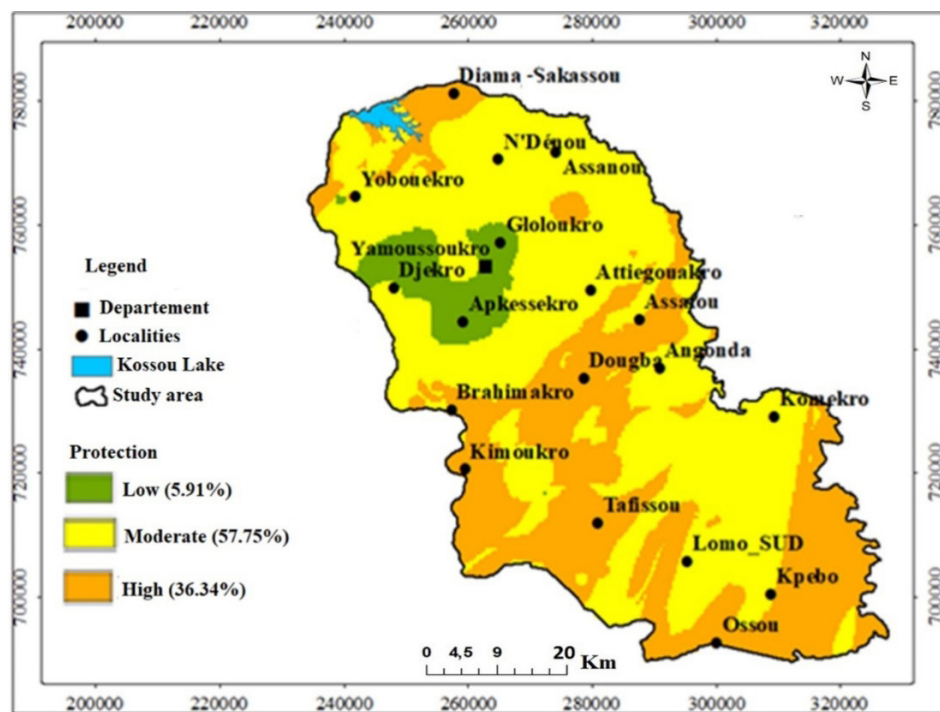


Figure 7. Thematic map of protection criteria.

Table 8. Vulnerability parameter statistics.

Paramter	Min	Max	Average	Standard deviation	Uncertainty
Protection	1.57	3.13	2.23	0.32	± 0.04
Reservoir	1	3.26	2.98	0.18	± 0.02
Infiltration	1	4	3.14	0.43	± 0.05
Sum	$Iv \cdot m = 8.35$			$\sum \Delta = 0.11$	
Error				$Er = 1.31\%$	

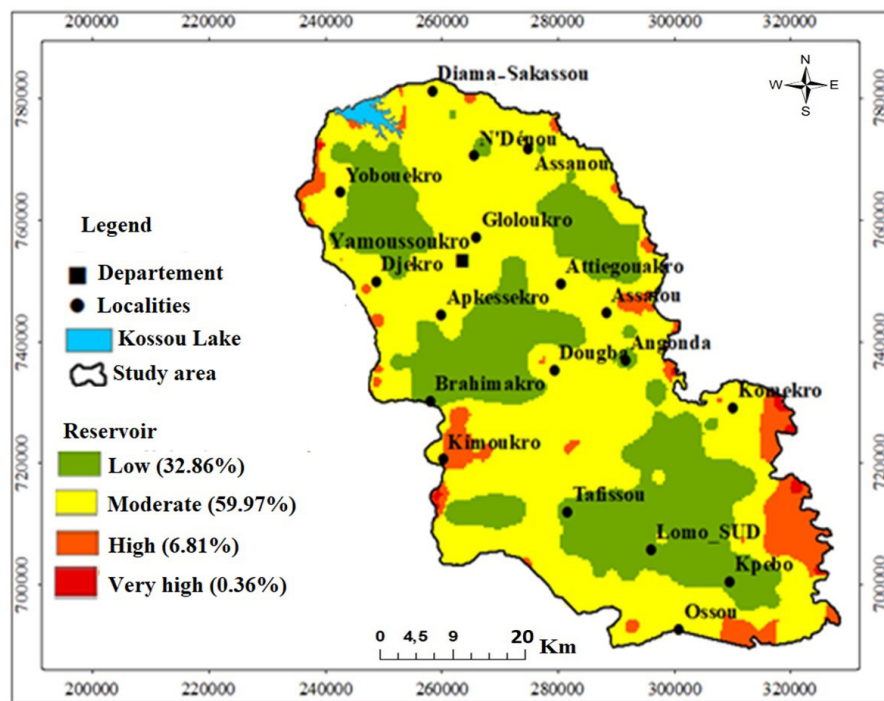


Figure 8. Thematic map of the rock or reservoir criterion.

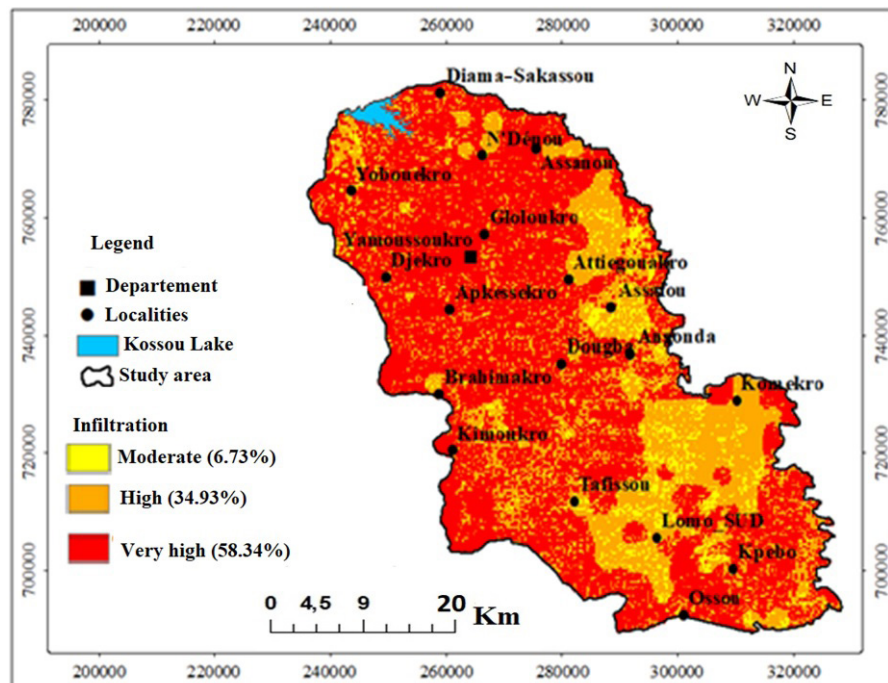


Figure 9. Thematic map for the infiltration criterion.

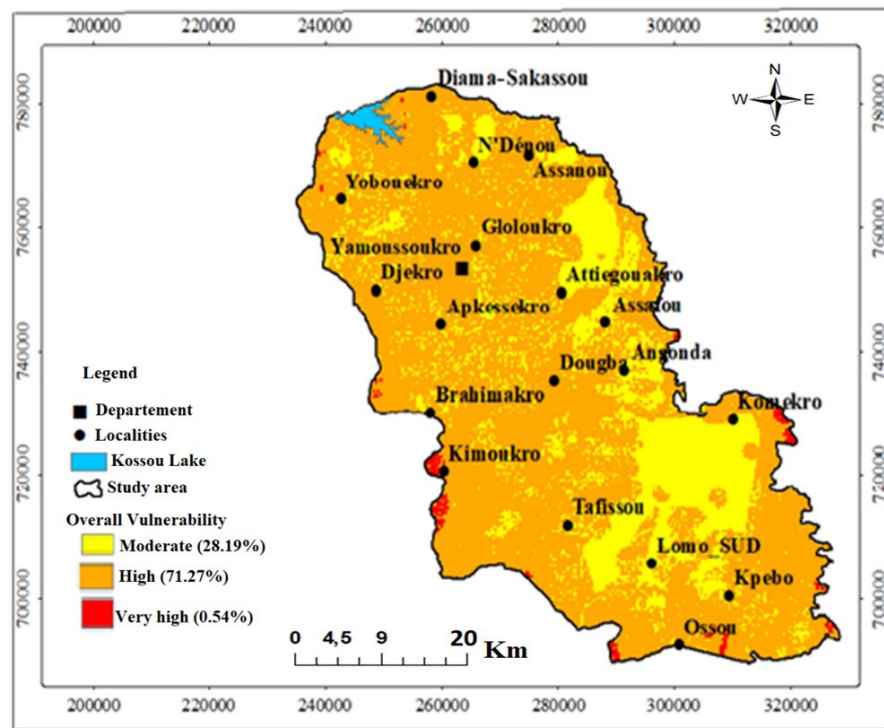


Figure 10. Map of overall vulnerability to groundwater pollution in the Yamoussoukro department.

the total surface area). This good groundwater availability could be due to high fracturing density, which would lead to good infiltration of water into the aquifer (Shankar & Mohan 2006, Doumouya *et al.* 2012, Mangoua *et al.* 2014). This good infiltration is also due to the abundance of rainfall, around 1300 mm/year, which constitutes the main source of recharge for the aquifer. Indeed, in humid tropical zones such as Côte d'Ivoire, aquifers are essentially fed by rainfall via surface infiltration (Yao *et al.* 2012). The poor and average availability classes obtained could be due to very steep slopes associated with high drainage densities, which accelerate water flow and slowing down infiltration into the water table (Shankar & Mohan 2006). These zones are not conducive to the formation of large underground reservoirs. Nevertheless, a borehole located at the right or intersection of open mega-fractures can provide exceptional flow rates, even though it is in a zone of poor or average availability. The predominance of zones with good and excellent groundwater availability could be attributed to the presence of essentially granitic formations. Indeed, according to N'Go *et al.* (2005), heterogeneous granites are the most productive lithological formations. The PaPRI method, specially designed for assessing intrinsic vulnerability, is based on structural factors and hydraulic behavior, in line with the concepts developed by Mangin (1975) for karsts. The P factor, which characterizes groundwater protection, covers all factors capable of acting as a first curtain to prevent pollutants from reaching the water table. The protection criterion map of the study area is dominated by the moderate vulnerability class, which covers 57.75% of the study area. In fact, the moderate thickness and nature of these layers, which result from the combination of soil layers, weathering and the unsaturated zone, could hinder the transport of pollutants. They could also reduce infiltration rates, thus preventing pollutants from reaching the groundwater table. Analysis of the "reservoir" map shows that the area is dominated by moderate permeability, covering around 59.97% of the surface area. This permeability can be

explained by moderate fracture density, since the reservoir rock is derived from the alteration of sound rock (mostly granitic and some gneiss). These results are in line with those of Dibi *et al.* (2015) and Kamenan *et al.* (2020), who indicate that in basement formations, the R criterion is highly dependent on fracturing and alteration, which affects the reservoir's hydrodynamic properties. The "infiltration" criterion, for its part, determines the ability to delay or accelerate infiltration. It is dominated by very high and high infiltration classes over the entire study area. These classes cover 93.27% of the study area. In these areas, drainage density is average with low slopes. However, slope remains the most important parameter, as the lower the slope, the more vulnerable the aquifer. This means that in low-slope areas, water remains in contact with the soil for longer, facilitating infiltration compared with steep-slope areas. Water is then rapidly evacuated, as shown by the work of Prasad *et al.* (2008), who demonstrated that the steeper the slopes and the greater the drainage density, the lower the probability of water infiltrating the water table, and vice versa. Finally, the vulnerability map highlights the high vulnerability class, which covers around 71.27% of the study area. This high level of vulnerability could be explained by the high density of fracturing, which makes underground geological formations highly permeable, as well as by their gentle slopes, which favor the infiltration of water from the surface into the groundwater. Added to this are the average thicknesses of the protective layers, which make vertical transport of the contaminant more or less straight forward. These results are similar to those of Dibi *et al.* (2013), Mangoua *et al.* (2020) and Kamenan *et al.* (2020), who highlighted the importance of soil type, indicating that the presence of a highly permeable soil associated with a shallow water table and high recharge would be a favorable condition for increasing vulnerability to aquifer pollution. The PaPRI method has produced results similar to those of several authors, including Dibi *et al.* (2015) and Mangoua *et al.* (2018), but presents some shortcomings in the production of vulnerability maps. These difficulties lie

mainly in the number of criteria to be taken into account and in the limits of the classes and ratings assigned to them (Murat 2000). Despite these various limitations, the vulnerability map remains reliable. The reliability of this map was tested by determining the margin of error on the vulnerability map, as done by Dibi *et al.* (2013). In the present study, the low value of the margin of error on each map testifies to both the good quality of the scores attributed to the various parameters and to the adaptation of this method to the study area. In fact, the margin of error calculated to assess the method was 1.31%. This margin of error is lower than that obtained by Kamenan *et al.* (2020) in the Lobo watershed at Nibéhibé. The margin of error obtained by these authors is 2.8% using the same method.

CONCLUSION

The identification of potential groundwater storage areas, based on GIS and multicriteria analysis, led to the conclusion that the Yamoussoukro department is rich in significant groundwater resources. The excellent and good classes cover around 67% of the area, indicating good water infiltration. This good infiltration of water throughout the department could explain the high availability, accessibility and exploitability of groundwater. The vulnerability of groundwater pollution in this department was mapped using the PaPRI intrinsic vulnerability method. This map was obtained by combining three criteria: protection, reservoir and infiltration. The area is dominated by the high vulnerability class, which occupies 71.27% of the total study zone area, with a margin of error of 1.31%, showing that the intrinsic vulnerability map is reliable. To protect groundwater in the department, it would be advisable to establish protection zones around boreholes to preserve groundwater quality. This study could be further improved by hydrogeochemical validation, which we plan to conduct in our upcoming studies.

Acknowledgments

The authors would like to thank all those people who helped them in the practical phase of this study. They also would like to express their gratitude to the editor of «*Bulletin de l'Institut Scientifique*» ACHAB Mohammed and the journal reviewer's prof. Kawtar BARGACH and prof. Abderrahime NOUYATI from the Scientific Institute of Rabat, for their significant contributions to the improvement of the manuscript.

REFERENCES

Ahoussi K.E. 2008. *Évaluation quantitative et qualitative des ressources en eau dans le Sud de la Côte d'Ivoire. Application de l'hydrochimie et des isotopes de l'environnement à l'étude des aquifères continus et discontinus de la région d'Abidjan-Agboville*. Thèse de Doctorat de 3^{ème} cycle, Université de Cocody, 283 p.

Arkoprovo B., Adarsa J. & Prakash H.S. 2012. Delineation of groundwater potential zones using satellite remote sensing and geographic information system techniques: a case study from Ganjam district, Orissa, India. *Research Journal of Recent Sciences*. 1(9), 59–66, <http://203.18.51.96:8080/jspui/bitstream/123456789/817/1/19-AB.pdf>.

Biémi J. 1992. *Contribution à l'étude géologique, hydrogéologique et par télédétection des bassins versants subsahariens du socle précambrien d'Afrique de l'Ouest : Hydrostructurale, Hydrodynamique, Hydrochimie et Isotopie des aquifères discontinus de sillons et aires granitiques de la haute Marahoué (Côte d'Ivoire)*. Thèse de Doctorat de 3^{ème}, Université de Cocody, 479 p.

Burrough P.A. 1986. Principles of geographic information systems for land resource assessment. Oxford Science Publications, New York, *Monographs on Soil and Resources Survey*, 12, 1-24.

Das S. & Pardeshi S.D. 2018. Integration of different influencing factors in GIS to delineate groundwater potential areas using IF and FR techniques: a study of Pravara basin, Maharashtra, India. *Applied Water Science*, 8, 7, 197. doi:<https://doi.org/10.1007/s13201-018-0848-x>.

Dibi B. 2008. *Cartographie des sites potentiels d'implantation des points d'eau dans le département d'Aboisso (Sud-Est de la Côte d'Ivoire) : Apport du SIG et de l'analyse multicritère*. Thèse de Doctorat de 3^{ème} cycle, Université de Cocody, 164 p.

Dibi B., Konan-W.A.B., Konan K.F. *et al.* 2013. Characterization of the origin of pollutants in groundwater from biostatistical tests: the case of catchment Ehania, south-eastern Côte d'Ivoire. *Journal of Water Resource and Protection*, 5, 12, 1178-1185.

Dibi B., Plagnes V., Konan-W.A.B. *et al.* 2015. Définition d'une méthodologie de dimensionnement des zones de protection des ouvrages de captage d'eaux souterraines en zone de socle. Cas de la zone test du bassin versant d'Ehania (Sud-Est de la Côte d'Ivoire). *20^{èmes} journées techniques du Comité Français d'Hydrogéologie de l'Association Internationale des Hydrogéologues*. « Aquifères de socle : le point sur les concepts et les applications opérationnelles », La Roche-sur-Yon (France), 8 p.

DHH 2001. Bilan diagnostique et redynamisation du dispositif de maintenance des pompes manuelles. Séminaire de réflexion sur la maintenance des pompes d'hydraulique villageoise, 47 p.

Doumouya I., Brou D., Kouassi I.K. *et al.* 2012. Modelling of favourable zone for the establishment of water points by geographical information system (GIS) multicriteria analysis (MCA) in the Aboisso area (South-east of Côte d'Ivoire). *Environmental Earth Sciences*, 67, 6, 1763-1780.

Dörfliger N. & Plagnes V. 2010. Cartographie de la vulnérabilité de l'aquifère karstique guide méthodologique de la méthode PaPRIKA. Rapport BRGM, Orleans, France, 100 p.

Dörfliger N. & Plagnes V. 2009. Cartographie de la vulnérabilité intrinsèque des aquifères karstiques. Guide méthodologique de la méthode PaPRIKA. ; BRGM RP-57527- FR, 105 p.

El Majorni Z. 2003. *Conception d'un système d'information à référence spatiale pour la gestion environnementale ; application à la sélection de sites potentiels de stockage de déchets ménagers et industriels en région semi-aride (Souss, Maroc)*. Thèse de Doctorat de 3^{ème}cycle, Université de Genève. Terre et Environnement, 42, 300 p.

INS (Institut National de la Statistique) 2021. Recensement Général de la population et de l'Habitat. Résultats globaux. 26 p.

Jourda J.P., Saley M.B., Djagoua E.V. *et al.* 2006. Utilisation des données ETM+ de Landsat et d'un SIG pour l'évaluation du potentiel en eau souterraine dans le milieu fissuré précambrien de la région de Korhogo (nord de la Côte d'Ivoire) : approche par analyse multicritère et test de validation. *Revue de Télédétection*, 5, 4, 339-357.

Kaliraj S., Chandrasekar N. & Magesh N.S. 2015. Evaluation of multiple environmental factors for site-specific groundwater recharge structures in the Vaigai River upper basin, Tamil Nadu, India, using GIS-based weighted overlay analysis.

Environmental Earth Sciences, 74, 5, 4355–4380. <https://doi.org/10.1007/s12665-015-4384-9>.

Kamenan Y.M. 2021. *Élaboration d'un modèle de protection des eaux souterraines en zone de socle : cas des aquifères du bassin versant de la Lobo à Nibéhibé (Centre-ouest de la Côte d'Ivoire)*. Thèse Unique, Université Jean Lorougnon Guédé, 170p.

Kamenan Y.M., Mangoua M.J., Dibi B. *et al.* 2020. Assessment of vulnerability to Groundwater Pollution in the Lobo Watershed at Nibéhibé (Central-West, Côte d'Ivoire). *Journal of Water Resource and Protection*, 12, 657-671.

Kanohin F. 2010. *Évaluation des ressources en eau de surface et souterraine dans un contexte de variabilité climatique dans la région de Daoukro (Nord-est de la Côte d'Ivoire)*. Thèse unique de Doctorat, Université Abobo-Adjamé, Abidjan, 146p.

Kavouri K., Plagnes V., Tremoulet J. *et al.* 2011. PaPRIKA: a method for estimating karst resource and source vulnerability-application to the Ousyse karst system (southwest France). *Hydrogeology Journal*, 19, 339–353.

Kindie A.T., Enku T., Moges M.A. *et al.* 2018. Spatial analysis of groundwater potential using GIS based multi criteria decision analysis method in Lake Tana Basin, Ethiopia. In *International Conference on Advances of Science and Technology*, 274, 439–456. doi:<https://doi.org/10.1007/978-3-030-15357-1-37>.

Koffi B., Sanchez M., Kouadio Z.A. *et al.* 2021. Evaluation of the impacts of climate change and land-use dynamics on water resources: the case of the Lobo River watershed: Central-Western Côte d'Ivoire. EGU General Assembly 2021 Author(s) 2021, EGU21: Gather Online (2021) 19–30 April 2021, doi:[10.5194/egusphere-egu21-506](https://doi.org/10.5194/egusphere-egu21-506).

Koffi B., Brou L.A., Kouamé J.O.K. *et al.* 2023. Impact of climate and land use/land cover change on Lobo reservoir inflow, West-Central of Côte d'Ivoire. *Journal of Hydrology: Regional Studies*, 47, 1-24. <https://doi.org/10.1016/j.ejrh.2023.101417>.

Kouadio K.J.O. 2022. *Modélisation du mode de recharge et du transfert des polluants des eaux souterraines du bassin versant de la Lobo à Nibéhibé (Centre-ouest de la Côte d'Ivoire)*. Thèse unique de Doctorat, Université Jean Lorougnon Guédé, 209 p.

Kouassi F.W., Mangoua M.J., Kouassi K.A. *et al.* 2017. Caractéristiques hydrogéochimiques des aquifères fissurés de la région d'Odienné, Nord-Ouest de la Côte d'Ivoire. *Afrique SCIENCE*, 13, 3, 30-42.

Magesh N.S., Chandrasekar N & Soundranayagam J.P. 2012. Delineation of groundwater potential zones in Theni district, Tamil Nadu, using remote sensing, GIS and MIF techniques. *Geoscience frontiers*, 3, 2, 189–196. <https://doi.org/10.1016/j.gsf.2011.10.007>.

Mahé G., Laraque A., Orange D. *et al.* 2001. Spatiotemporal variations in hydrological regimes within Central Africa during the XXth century. *Journal of Hydrology*, 245(1-4), 104-117.

Mangin A. 1975. *Contribution à l'étude hydrodynamique des aquifères karstiques [Contributions to the Hydrodynamics of Karst Aquifers]*. Thèse de Doctorat de 3^{ème} cycle, Université de Dijon, 124 p.

Mangoua M.J., Dibi B., Koblan E.W. *et al.* 2014. Map of potential areas of groundwater by the multi-criteria analysis for the needs for water of the Baya's catchment basin (East of Côte d'Ivoire). *African Journal Agricultural Research*, 9, 45, 3319-3329.

Mangoua M.J., Konan K.S., Kouamé K.I. *et al.* 2018. Évaluation de la vulnérabilité à la pollution des eaux souterraines du département de Tiassalé (Sud de la Côte d'Ivoire). *Environmental and water sciences public health & territorial intelligence*, 2, 2, 46-54.

Mangoua O.M.J., Kouassi K.A., Kouassi W.F. *et al.* 2020. Assessment of groundwater pollution in department of Odienné (North-West Côte d'Ivoire). *African Journal of Science, Technology, Innovation and Development*, 12, 3, 297-303.

Murat V. 2000. *Étude comparative des méthodes d'évaluation de la vulnérabilité intrinsèque des aquifères à la pollution : Application aux aquifères granulaires du Piémont laurentien*. Mémoire de maîtrise, Institut National de la recherche scientifique-Géosciences, Québec (Canada), 127 p.

Nagarajan M. & Singh S. 2009. Assessment of groundwater potential zones using GIS technique. *Journal of the Indian Society of Remote Sensing*, 37, 1, 69-77. <https://doi.org/10.1007/s12524-009-0012-z>.

N'guessan K.A., Kouassi A.M., Gnaboa R. *et al.* 2014. Analyse de phénomènes hydrologiques dans un bassin versant urbanisé : cas de la ville de Yamoussoukro (Centre de la Côte d'Ivoire). *Larhyss Journal*, 17, 135-154.

N'go Y.A., Gone D.L., Savane I. *et al.* 2005. Potentialités en eaux souterraines des aquifères d'Agboville (Sud-Ouest de la Côte d'Ivoire) : Caractérisation hydro-climatique et physique. *Afrique Science: Revue Internationale des Sciences et Technologie*, 01, 1, 127-144.

Pinto D., Shrestha S., Babel M.S. *et al.* 2015. Delineation of groundwater potential zones in the Comoro watershed, Timor Leste using GIS, remote sensing and analytic hierarchy process (AHP) technique. *Applied Water Science*, 7, 1, 503–519. <https://doi.org/10.1007/s13201-015-0270-6>.

Prasard R.K., Mondal N.C., Pallavi B. *et al.* 2008. Deciphering potential groundwater zone in bard rock through the application of GIS. *Environment of Geology*, 55, 467-475.

Rajasekhar M., Sudarsana Raju G., Bramaiah C. *et al.* 2018. Delineation of groundwater potential zones of semi-arid region of YSR Kadapa District, Andhra Pradesh, India using RS, GIS and analytic hierarchy process. *Remote Sensing of Land*, 2, 2, 76–86. <http://dx.doi.org/10.21523/gcj1.18020201>.

Raju R.S., Raju G. S & Rajasekhar M. 2019. Identification of groundwater potential zones in Mandavi River basin, Andhra Pradesh, India using remote sensing, GIS and MIF techniques. *HydroResearch*, 2, 1-11. <https://doi.org/10.1016/j.hydres.2019.09.001>.

Saaty T.L. 2008. Decision making with the analytic hierarchy process. *International Journal of Services Sciences*, 1, 1, 83-98.

Saley M.B. 2003. *Système d'informations à référence spatiale, discontinuités pseudo-images et cartographies thématiques des ressources en eau de la région semi-montagneuse de Man (Ouest de la Côte d'Ivoire)*. Thèse Doctorat de 3^{ème} cycle, Université de Cocody, 209 p.

Sashikkumar M.C., Selvam S., Kalyanasundaram V.L *et al.* 2017. GIS based groundwater modeling study to assess the effect of artificial recharge: a case study from Kodaganar river basin, Dindigul district, Tamil Nadu. *Journal of the Geological Society of India*, 89, 1, 57-64. <https://doi:10.1007/s12594-017-0558-2>.

Savané I. 1997. *Contribution à l'étude géologique et hydrogéologique des aquifères discontinus du socle cristallin d'Odienné (Nord-ouest de la Côte d'Ivoire) : apport de la télédétection et d'un système d'information hydrogéologique à référence spatiale*. Thèse de Doctorat d'Etat, Université de Cocody, 398 p.

Shankar R.M.N & Mohan G. 2006. Assessment of the groundwater potential and quality in the Bhatsa and Kalu river basins of Thane district, western Deccan Volcanic Province of India. *Environmental Geology*, 49, 990-998.

Siddi R.R., Sudarsana R. G., Ravikumar *et al.* 2016. Applications of Remote Sensing and GIS, For Identification of Groundwater Prospecting Zones in and around Nandalur, YSR District. *IJEP*, 36, 4, 293-304.

Sinan M. & Razack M. 2008. An extension to the DRASTIC model for assessing groundwater vulnerability to pollution: application to the Haouz aquifer of Marrakech (Morocco). *Environmental Geology*, 57, 349-363.

Thapa R., Gupta S., Guin S. *et al.* 2017. Assessment of groundwater potential zones using multi-influencing factor (MIF) and GIS: a case study from Birbhum district, West Bengal. *Applied Water Science*, 7, 7, 4117-4131. <https://doi.org/10.1007/s13201-017-0571-z>.

WHO. 2011. Guidelines to Drinking-water Quality (fourth edition). ISBN 978 92 4 154815 1 (NLM classification: WA 675), 564 p.

Yao A.B., Goula B.T.A., Kane A *et al.* 2016. Cartographie du potentiel en eau souterraine du bassin versant de la Lobo (Centre-ouest de la Côte d'Ivoire). *Hydrological Sciences Journal*, 61, 5, 856-867.

Yao A.B., Goula B.T.A., Kouadio Z.A. *et al.* 2012. Analyse de la variabilité climatique et quantification des ressources en eau en zone tropicale humide. Cas du bassin versant de la Lobo au Centre-Ouest de la Côte d'Ivoire. *Revue Ivoirienne des Sciences et Technologies*, 19, 136-157.

Youan Ta M., Lasm T., Jourda J.P. *et al.* 2011. Cartographie des eaux souterraines en milieu fissuré par analyse multicritère Cas de Bondoukou (Côte-d'Ivoire). *Revue internationale de géomatique*, 21, 1, 43-71.

Manuscrit reçu le 06/04/2025
 Version révisée acceptée le 23/10/2025
 Version finale reçue le 27/11/2025
 Mise en ligne le 02/01/2026